NASA Technical Memorandum 79136

COMBINED PRESSURE AND TEMPERATURE
DISTORTION EFFECTS ON INTERNAL FLOW
OF A TURBOFAN ENGINE

W. M. Braithwaite and Ronald H. Soeder
Lewis Research Center
Cleveland, Ohio

COMBINED PRESSURE AND TEMPERATURE DISTORTION EFFECTS
ON INTERNAL FLOW OF A TURBOFAN ENGINE

by W. M. Braithwaite and Ronald H. Soeder
National Aeronautics and Space Administration
Lewis Research Center
Cleveland, Ohio 44135

Abstract

An experimental investigation was conducted, and is herein reported, to obtain an additional data base for improving and verifying a computer simulation developed by an engine manufacturer. The multisegment parallel compressor simulation was designed to predict the effects of steady-state circumferential inlet total-pressure and total-temperature distortions on the flows into and through a turbofan compression system. It also predicts the degree of distortion that will result in surge of the compressor. Previous investigations have dealt mainly with the effects of total-pressure distortions. The investigation reported herein deals with the effect of combined 180° "square-wave" distortion patterns of total pressure and total temperature in various relative positions. The observed effects of the combined distortion on a unitary bypass ratio turbofan engine are presented in terms of total and static pressure profiles and total temperature profiles at stations ahead of the IGV (inlet guide vanes) as well as through the fan-compressor system. These observed profiles are compared with those predicted by the complex multisegment model. The effects of relative position of the two components comprising the combined distortion on the degree resulting in surge are also presented. Certain relative positions required less combined distortion than either a temperature or pressure distortion by itself.

Nomenclature

A   average operating point for PCM, Fig. 15

D   inlet duct diameter

HPC   high pressure compressor

IGV   inlet guide vanes

L   distance upstream of IGV

LPC   low pressure compressor

max   maximum pressure or temperature in profile

min   minimum pressure or temperature in profile

N_1 low rotor (fan) speed

N_{1R2} low rotor speed corrected to station 2

P_S static pressure

P_T total pressure

PCM   parallel compressor model

R   effective mean radius of IGV

RNI   Reynolds number index = $\delta/\varphi \cdot \sqrt{\theta}$

S   stall point for PCM, Fig. 14

T   total temperature

U   unstall operating point for PCM, Fig. 15

v   velocity

v_a axial velocity

WACR   corrected core airflow

WATR   corrected total airflow

α radial (pitch) flow angle, Fig. 4

β circumferential (yaw) flow angle, Fig. 4

δ ratio of total pressure to sea level

Δ difference in numbers

θ ratio of total temperature to sea level

φ ratio of viscosity to sea level value

Subscripts:

AV   average

A   station A - downstream of screen

I-4   stations in compressor

IGV   IGV station

PCM   parallel compressor model

Introduction

The effect of inlet flow distortion on the performance and stability of aircraft gas turbine engines has long been an important consideration in development programs. In support of this, an extensive program has been undertaken by the Lewis Research Center to evaluate the effects of inlet flow distortion on the various types of engines. This paper presents the results obtained with combined 180° square wave total pressure and total temperature distortions imposed on the inlet flow of a low bypass turbofan engine.

In an effort to reduce the amount of experimental data required for the development of new engines, it is proposed that analytical models based on experimental data be developed. Such models should be capable of predicting the effects of distortion on engine flow characteristics and stability. Preliminary estimates of distortion sensitivity should be obtainable using the design characteristics. As more data are obtained the model would become more reliable and thus reduce the uncertainties inherent in engine development.

Several such models have been developed by the engine manufacturers.[1-5] The model of the TF30[1] was fine tuned using total pressure distortion data generated during Lewis testing to match the particular characteristics of the engine being used.[6-8] This refined model was then used to predict the results of a proposed investigation of combined pressure and temperature distortions.

Development of these models require experimental data showing the characteristics of the flow into and through the compressor system. The characteristics include the usual pressure and temperature profiles. Also of interest is the direction and magnitude of the flow, or velocity vector, especially at the compressor inlet. Previous work has shown the effects of total pressure distortion on

1

turbofan engines, and both pressure and temperature distortions on turbojet engines.[9-11] An experimental program was conducted using a TF30-P-3 turbofan engine to obtain better definition of the flow ahead of the inlet and through the compressor system. In addition, it was desired to evaluate the effectiveness of the model in predicting the flow characteristics with combined pressure and temperature distortions.

Apparatus

The engine used for this investigation was a TF30-P-3. It was installed in a 7.3 meter diameter altitude test chamber at the Lewis Research Center in a direct connect mode as shown in Fig. 1. Two devices were used to generate the combined pressure and temperature distortions. The total pressure distortion reported herein was generated with a 50% blockage screen mounted in the inlet duct approximately one duct diameter ahead of the compressor face and is shown in Figs. 2(a) and 3. This screen holder was capable of indexing the screen, and thus the distortion. The total temperature distortion was generated by means of the gaseous hydrogen burner, Fig. 2(b), mounted approximately six duct diameters ahead of the compressor face. The burner mounting permitted rotation of the burner $\pm30°$ from the position shown, Fig. 2(b). This movement, coupled with the indexing of the burning quadrants, permitted the indexing of the distortions in $30°$ steps. Thus there was a 12 fold increase in resolution of the circumferential profiles.

The engine was instrumented in such a manner that circumferential profiles of total pressure and temperature and static pressure could be determined in front of and through the compression system. These profiles were measured just downstream of the distortion screen (station A), at the inlet guide vanes (IGV), and in the 1st, 3rd, 6th, 9th, 12th, and 16th stage stators. The locations and number of probes at each station is shown in Fig. 3. Two rows of static pressure taps extended from the distortion screen (station A) to the IGV and were located at approximately $120°$ from the top of the duct on the inner and outer annular wall.

Additional instrumentation was installed in the IGV to measure the angle between the flow vector and the axial direction. The instrumentation used was the five point probe as described in Ref. 12 and shown in Fig. 4(a). The indicated pressure difference between the outer probes as a percentage of the approximate dynamic head is proportional to the flow angle. The flow angle in the circumferential direction was also measured in the boundary layer using the rakes shown in Figs. 4(b) and (c).

The effect of combined pressure and temperature distortions on the stability limits was determined by slowly increasing the temperature distortion with the screen in place until stall was reached. Since the screen could be indexed independently of the burner, the effects of the relative position of the distortions could be investigated.

During the various phases of the investigation the following test conditions were maintained. The Reynolds Number Index in the undistorted sector of the inlet was maintained at 0.5 with the temperature being 289 K. The low rotor speed of 90% of

military and 100% rated jet nozzle area were used. A large amplitude pressure distortion was necessary to keep the distortion more discernable as it attenuated within the engine. Therefore, the 7th stage compressor bleed was open during the profile mapping but was closed for the stability limit part of the investigation.

Results and Discussion

The effect of inlet flow distortion on the performance of a turbofan engine will be discussed in three sections. The first will describe the flow between the screen and the IGV; the second will describe the flow through the compression system; and the last will present the effects of the combined distortion and its orientation on the compressor stability limits.

Inlet Flow

For ease in describing the flows between the screen and the IGV, the effects of the total pressure and total temperature distortions will be treated separately. The parallel compressor theory, as will be discussed later, requires a specific mass-flow profile at the engine face. But the flow behind the distortion screen does not match this profile as there is a rather severe flow distortion just downstream of the screen. As shown in Refs. 1 and 13, a static pressure distortion is generated by the attenuation of this flow distortion between the screen and the IGV.

The total pressure distortion generated by the 50% blockage screen is shown in Fig. 5. The 14% ((max-min)/av) total pressure distortion level was not attenuated between the screen and the IGV. However, the circumferential extent of the distortion was less at the IGV than just behind the screen. The static pressure distortion at station A was approximately 2% and increased to 9% at the IGV. Combining the total and static pressures and there being no total temperature distortion, the distribution of corrected mass flow per area was calculated and is shown in Fig. 5(c). The mass flow distortion was about 60% at the station A and decreased to 35% at the IGV.

In the case of total temperature distortion, the corrected mass flow distribution should be relatively uniform at station A as there is no total pressure distortion nor obvious means of supporting a static pressure distortion. But the simple parallel compressor model requires a corrected mass flow profile with its associated static pressure profile. The effects of total temperature distortion are shown in Fig. 5(d). In this case the total pressure distribution is uniform. It can be seen that the total temperature profile is not as square as was the total pressure profile. There appears to be an increase in temperature downstream of the plate dividing the two burning quadrants. The temperature distortion ((max-min)/av) at station A was approximately 32% and decreased only slightly at the IGV to 28%. There was almost no static pressure distortion at station A and only 3% at the IGV. The resultant mass flow distortion was approximately 6% at station A and 12% at the IGV.

2

The buildup of static pressure distortion as the flow approaches the IGV was shown to follow an exponential relationship as given in Refs. 1 and 13 for imposed total pressure distortions. The static pressure distortions resulting from total temperature and combined pressure/temperature distortions also follow this relationship so is shown in Fig. 6. There is good agreement between the three sets of data. They are slightly higher than the exponential fit near station A, but the levels of pressure are low and there is probably some effect of the distortion devices not accounted for by the exponential fit.

One consequence of the static pressure distortion ahead of the compressor has been the apparent disagreement between the measured and predicted mass flow distributions. This was especially true for the total temperature distortions. The insert on Fig. 7 shows a simple parallel compressor model representation of a temperature distortion. The flows for parallel compressor units S & U are significantly different. This difference would require a significant static pressure profile. The predicted static pressure distortion can be adjusted for the distance, L_2, that station 2 is ahead of the IGV using the exponential relationship,

$$\frac{\left(\Delta P_s\right)_2}{\left(P_{T2}\right)_{AV}} = \frac{\left(\Delta P_s\right)_{IGV}}{\left(P_{T2}\right)_{AV}} \times e^{-L_2/R}$$

a modified version of the expression of Ref. 1. The results of this adjustment is shown in Fig. 7. The agreement is good for all the various configurations shown.

The angle that the flow makes with the axial direction at the IGV is shown in Fig. 8. This angle was measured approximately 2.5 cm ahead of the IGV, about half way between the tip and the hub of the blade. The positive angle is defined as the one with a component in the direction of engine rotation. It can be seen that the total pressure distortion induced a positive flow angle at the leading edge of the distortion, or low pressure region, and a negative angle at the exit of this region. This implies that there is flow into the distorted region. From Fig. 5(b) it can be noted that this also is a region of low static pressure. For the total temperature distortions, the flow angle is negative at the leading edge and positive at the trailing edge of the heated section of the inlet. This is the reverse of that for the pressure distortion and implies that the flow is out of the heated region. The static pressure is higher in the heated sector, Fig. 5(e), and thus the circumferential flow is again from the high to the low static pressure region. It can also be noted that the largest flow angle is in the region of the steepest total pressure gradient, that is, at the edge of the distortion, and the minimum angles are in the center of the distorted and undistorted regions where there is no total pressure gradient. The magnitude of the flow angle is much greater for the pressure distortion than for the temperature distortion. There is a 30° flow angle variation for the 14% pressure distortion and an 8° variation for the 28% temperature distortion. Compared on the basis of the static pressure distortions, there is a 30° variation for a 9% static pressure distortion associated with the total pressure distortion and an 8° variation for the 3% static pressure distortion which is associated with the total tempera-

ture distortion. The flow angle, therefore, seems to be a function of the static pressure distortion.

Internal Flow

A combined total pressure and total temperature distortion was selected to demonstrate the capability of the model to describe internal flow characteristics. The 180° total pressure distortion was oriented in the lower half of the inlet, Fig. 9. The total temperature distortion was oriented such that the high temperatures were in the right hand side, Fig. 9. A compressor blade would thus pass through 90° of low temperature-high pressure followed by 90° of low temperature-low pressure, followed by 90° of high temperature-low pressure, and then 90° of high temperature-high pressure.

The fan inlet temperature and pressure profiles were then put into the multisegment parallel compressor mode.[2] The predictions from the program are represented by the lines on Fig. 9 for several key stages in the compressor. Reasonable agreement was achieved between the model and the experimental data. The predicted swirl or rotation of the center of both the total pressure and temperature distortions as they pass through the compressor can be seen here and in Fig. 10. This swirl can lead to some incorrect readings if it is not properly accounted for when specifying instrumentation for control sensors and/or research projects.

The TF30 model also predicted the inlet flow angle at the IGV, Fig. 11, and they are compared with the measured angles. The model predicted greater angles than measured in the undistorted regions with a maximum variation in the measured angle of 16° as compared to 19° for the model.

The measured attenuations of the total pressure and total temperature distortions and static pressure distortion are compared with those predicted by the model in Fig. 12. The experimental data exhibit a greater spread than does the model. However, the agreement was within 3.0% of the average temperature. The pressure distortions are attenuated as they pass through the compressor going from 9% to about 1% at the compressor exit. The total temperature distortion, however, was not attenuated to the same degree, going from 9% to 7%. The model had predicted a slightly greater attenuation to 5%.

The effects of relative position are shown in Fig. 13. The most persistent distortion occurs when the high temperature and low pressure are in the same 180° sector and the most attenuated occurs when they are opposed. The two 90° overlapping cases fit in between the extremes.

Stability Limits

The results of the experimental investigation into the combined distortions which resulted in compressor stall are presented in Fig. 14. Included on this figure are data obtained using airjets to generate the combined distortion. The amount of pressure distortion required to stall the compression system is shown as a function of various levels of temperature distortion. Two regions are shown on the figure; one in which the high tempera-

ture is aligned with the low pressure region (negative delta T), and one in which the high temperature and low pressure are opposed to each other (positive delta T). Starting with a negative delta T, pure temperature distortion, it is seen that as the temperature distortion decreases, larger total pressure distortions are required to stall the compression system until a pure pressure distortion is obtained. If the temperature distortion is now located in the opposite side of the inlet, increasing levels of pressure distortion are required for increasing temperature distortions.

A second limit line is observed for the opposed distortions. For a pure-temperature distortion, the distortion required to stall the engine is the same on either side of the engine. There is a stall region to the right of this point.

It was shown in Ref. 9 that the relative positions of these distortions would have a significant effect on the stability limits of the turbojet engine. It was predicted in Ref. 2 that a near linear inverse relationship xists between the levels of pressure distortion and temperature distortion required to stall the compression system. When aligned, the simple parallel compressor model depicts the two units as operating at points SII and UII on Fig. 15(a). Point AII is the average operating point. The -I points represent temperature distortion only; the II points represent combined distortion; and the III points represent pure pressure distortions. As point S, representing the stalling parallel compressor unit, moves from point SI to SIII, the temperature distortion is decreasing and the pressure distortion increasing. Figure 15(b) represents the case where the distortions are in opposite sides on the inlet. In this case we start with the pure pressure distortion as represented by SIII - UIII. As the temperature distortion increases, the point U moves from UIII to UI. The stall is in the pressure distorted unit, SI and SIII. There exists a second possibility, however. This is represented by SII - UII and in this case the stall occurs in the temperature distorted unit. It can be seen that there is only a small pressure distortion for this case.

The experimental data were obtained at an inlet RNI = 0.5 whereas the model prediction was for an RNI = 1.0. Based on previous experience, this difference in RNI would result in the model overpredicting the distortion level by approximately 2% for both total pressure and total temperature. Thus, the experimental data and the predicted limits agree reasonably well considering the complexity of the "T" compressor, that is, one having a fan-low unit on the same rotor spool. It is also difficult to accurately measure the temperature distortions due to the peaked profile as mentioned earlier. These peaks could be missed by the few rakes available during dynamic stability testing.

Concluding Remarks

Presented are the flow characteristics obtained experimentally for the compression system of a 2-spool turbofan engine operating with 180° combined pressure and temperature distortion in the inlet flow. The analytical model of Ref. 1 was used for pretest predictions of the results that these distortions and their relative positions would have on the engine flow characteristics and

the limiting distortion values. The model was first "tuned" to the particular engine using experimentally determined total pressure distortion data.

1. The was good agreement between the model and the tota -pressure and total-temperature profile data.

2. There was good agreement on the static pressure distortion build-up between the screen position and the IGV.

3. The agreement between the measured and predicted flow angles at the IGV was satisfactory.

4. The model predicted the trends obtained with the combined pressure and temperature distortions at the limiting values. For aligned high temperature and low pressures, the pressure distortion required to stall the compressor increased as the temperature distortion decreased. For the opposed high temperature-low pressure case, the required pressure distortion increased as the temperature distortion increased. At higher temperature distortions, a lower limiting pressure distortion was found. The simple parallel compressor theory predicted this limit as the temperature dominated limit, the upper instability being the pressure dominated limit.

5. Indexing of the distortion past the instrumentation provided good resolution for the internal profiles.

The model used in this program was capable of predicting the effects of total pressure, total temperature and combined total pressure-total temperature distortions in terms of flow profiles, inlet flow angles and attenuation of the distortions through the compressor system. It was also capable of predicting the ends of the limiting values experienced with various orientations of the combined distortions. The next step would be to insert the characteristics of a different compression system into the model. This is being done by Pratt & Whitney under NASA Contract NAS3-20835 and predictions are being made for a proposed distortion investigation using the F100 turbofan engine.

References

1. Mazzawy, R. S. and Banks, G. A., "Modeling and Analysis of the TF30-P-3 Compressor System with Inlet Pressure Distortion," Pratt and Whitney Aircraft, East Hartford, Conn., PWA-5302, April 1976. (NASA CR-134996)

2. Mazzawy, R. S. and Banks, G. A., "Circumferential Distortion Modeling of the TF30-P-3 Compressor System," Pratt and Whitney Aircraft, East Hartford, Conn., PWA-5448, Jan. 1977. (NASA CR-135124)

3. Mazzawy, R. S.; and Banks, G. A.; and Weber, C. R.: "Compressor Critical Response Time Determination Study." AFAPL-TR-76-45, June 1976.

4. Tesch, W. A. and Steenken, W. G., "Blade Row Dynamic Digital Compressor Program. Vol. 1: J85 Clean Inlet Flow and Parallel Compressor Models," General Electric Co., Cincinnati Ohio, R75AEG406, May 1976. (NASA CR-134978)
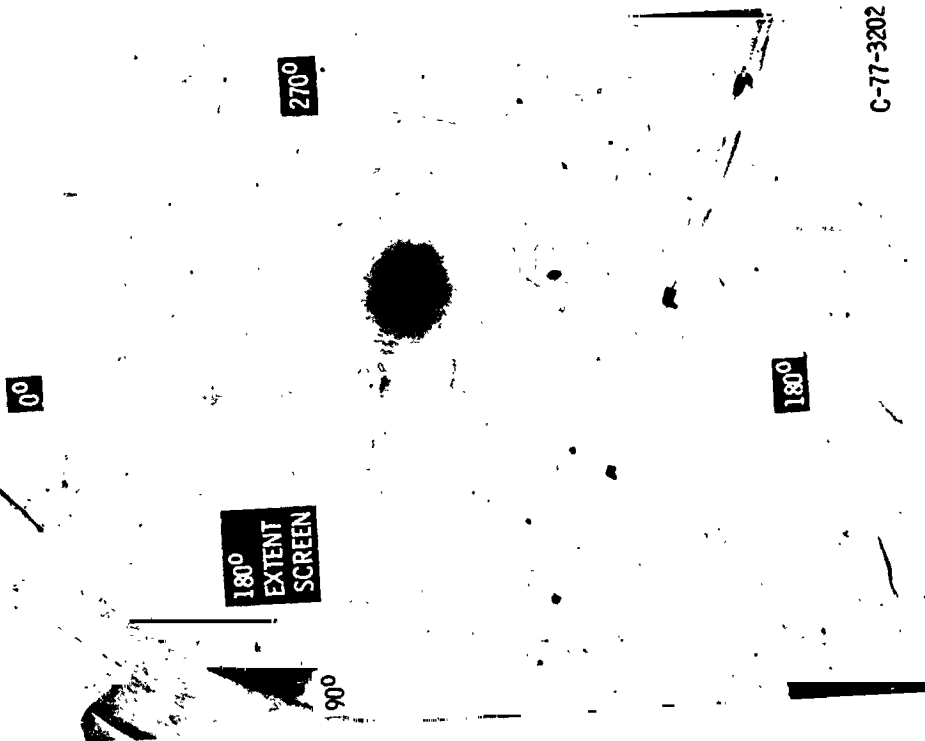
5. Tesch, W. A. and Steenken, W. G., "Blade Row
   Dynamic Digital Compressor Program. Vol. II:
   J85 Circumferential Distortion Model, Effect
   of Stator Characteristics, and Stage Charac-
   teristics Sensitivity Study," General Electric
   Co., Cincinnati, Ohio, R76AEG484, July 1978.
   (NASA CR-134953)

6. Braithwaite, W. M., "Experimental Evaluation of
   a TF30-P-3 Turbofan Engine in an Altitude
   Facility: Effect of Steady-State Temperature
   Distortion," NASA TM X-2921, 1973.

7. Evans, D. G., deBogdan, C. E., Soeder, R. H.,
   and Pleban, E. J., "Some Comparisons of the
   Flow Characteristics of a Turbofan Compressor
   System With and Without Inlet Pressure Distor-
   tion," NASA TM X-71574, 1974.

8. deBogdan, C. E., Dicus, J. H., Evans, D. G.,
   and Soeder, R. H., "Effect of a 180° Extent
   Inlet Pressure Distortion on the Internal
   Flow Conditions of a TF30-P-3 Engine," NASA
   TM X-3267, 1975.

9. Braithwaite, W. M., Graber, E. J., Jr., and
   Mehalic, C. M., "The Effect of Inlet Tempera-
   ture and Pressure Distortion on Turbojet Per-
   formance," NASA TM X-71431, 1973. Also AIAA
   Paper 73-1316, Nov. 1973.

10. Graber, E. J., Jr. and Braithwaite, W. M.,
    "Summary of Recent Investigations of Inlet
    Flow Distortion Effects on Engine Stability,"
    NASA TM X-71505, 1974. Also AIAA Paper
    74-236, Jan. 1974.

11. deBogdan, C. E., Moss, J. E., Jr., and
    Braithwaite, W. M., "Internal Flow Character-
    istics of a Multistage Compressor With Inlet
    Pressure Distortion," NASA TM X-3446, 1977.

12. Dudzinski, T. J. and Krause, L. N., "Flow-
    Direction Measurement with Fixed-Position
    Probes," NASA TM X-1904, 1969.

13. Plourde, G. A. and Stenning, A. H., "Attenua-
    tion of Circumferential Inlet Distortion in
    Multistage Axial Compressors," Journal of Air-
    craft, Vol. 5, May-June 1968, pp. 236-242.

270°

0°

180°
EXTENT
SCREEN

90°

180°
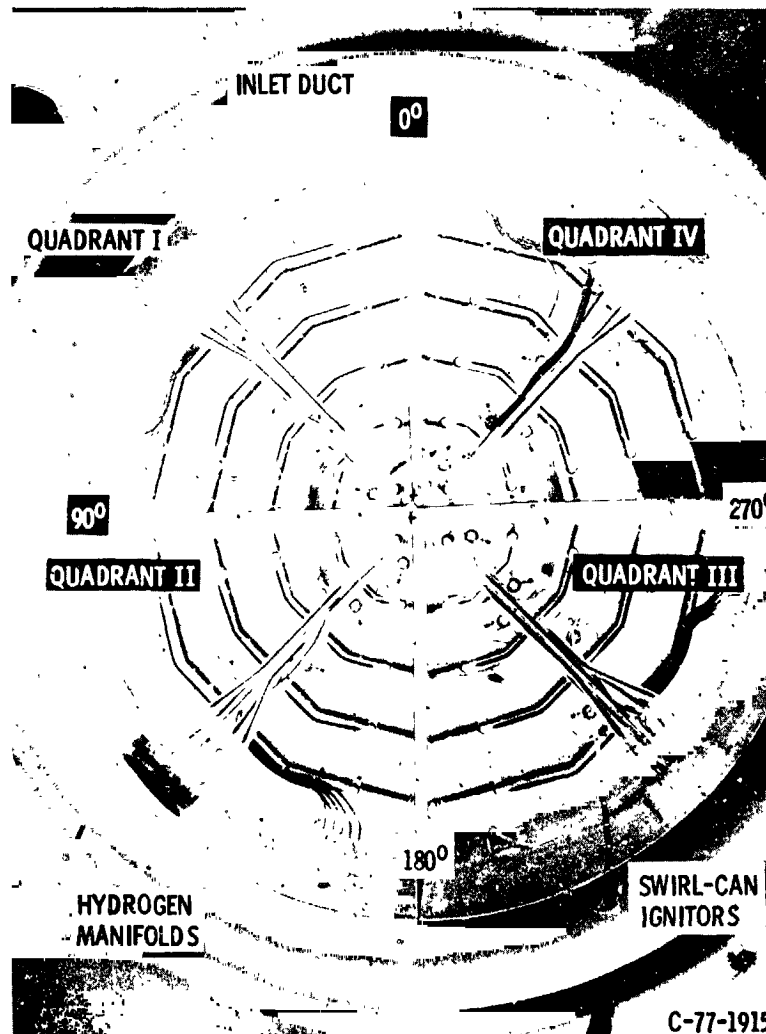
C-77-3202

(a) ROTATING SCREEN ASSEMBLY, VIEWED IN THE DIRECTION
OF THE ENGINE INLET.

Figure 2. – Distortion generating devices.

C-77-591

Figure 1. – TF30-P-3 Engine in altitude test chamber.

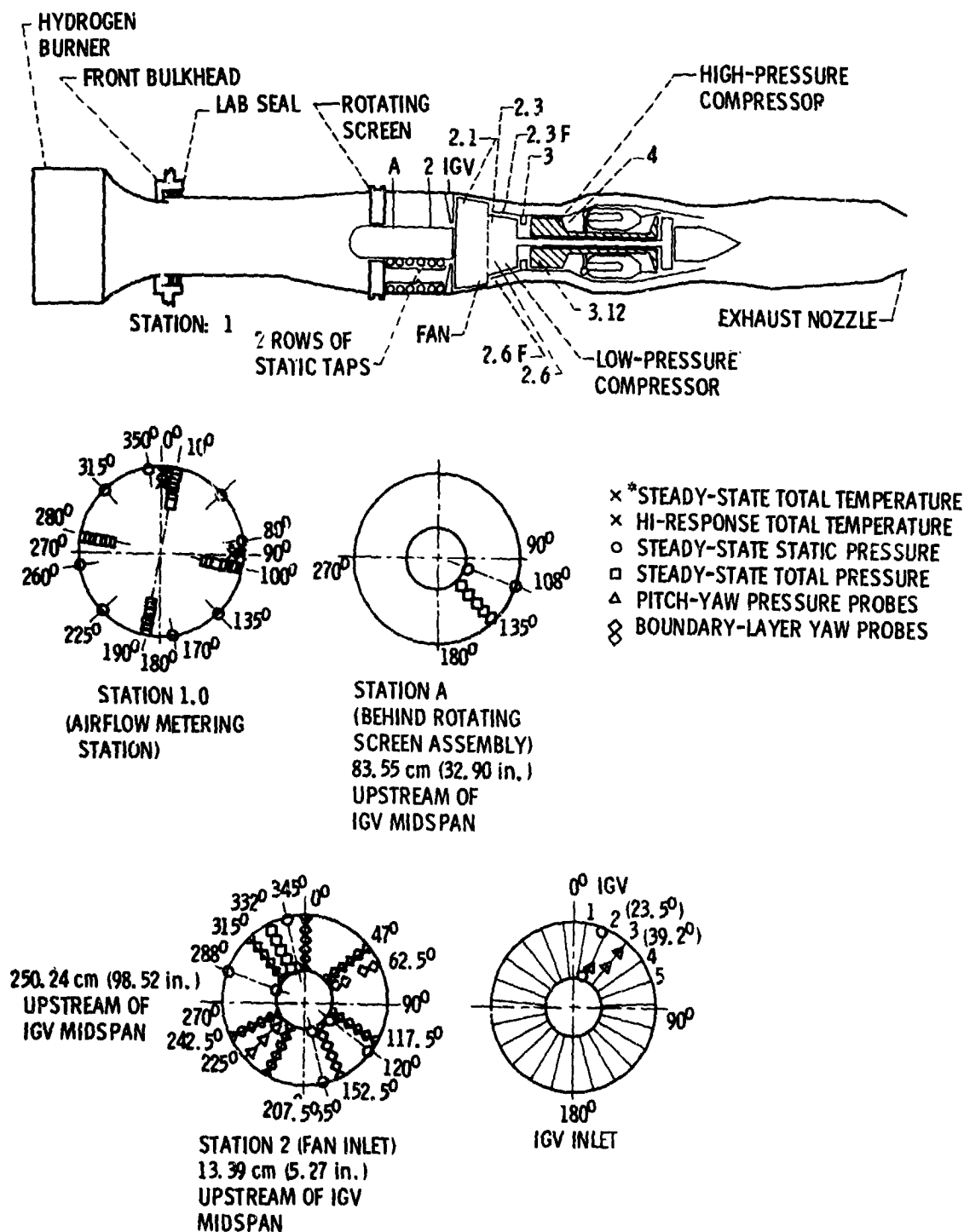(b) GASEOUS-HYDROGEN-FUELED BURNER VIEWED IN THE DIRECTION OF ENGINE INLET.

Figure 2. -Concluded.

Figure 3. – Instrumentation layout for TF30-P-3 turbofan engine.
(Instrumentation stations viewed looking upstream.)

STATION 2.1
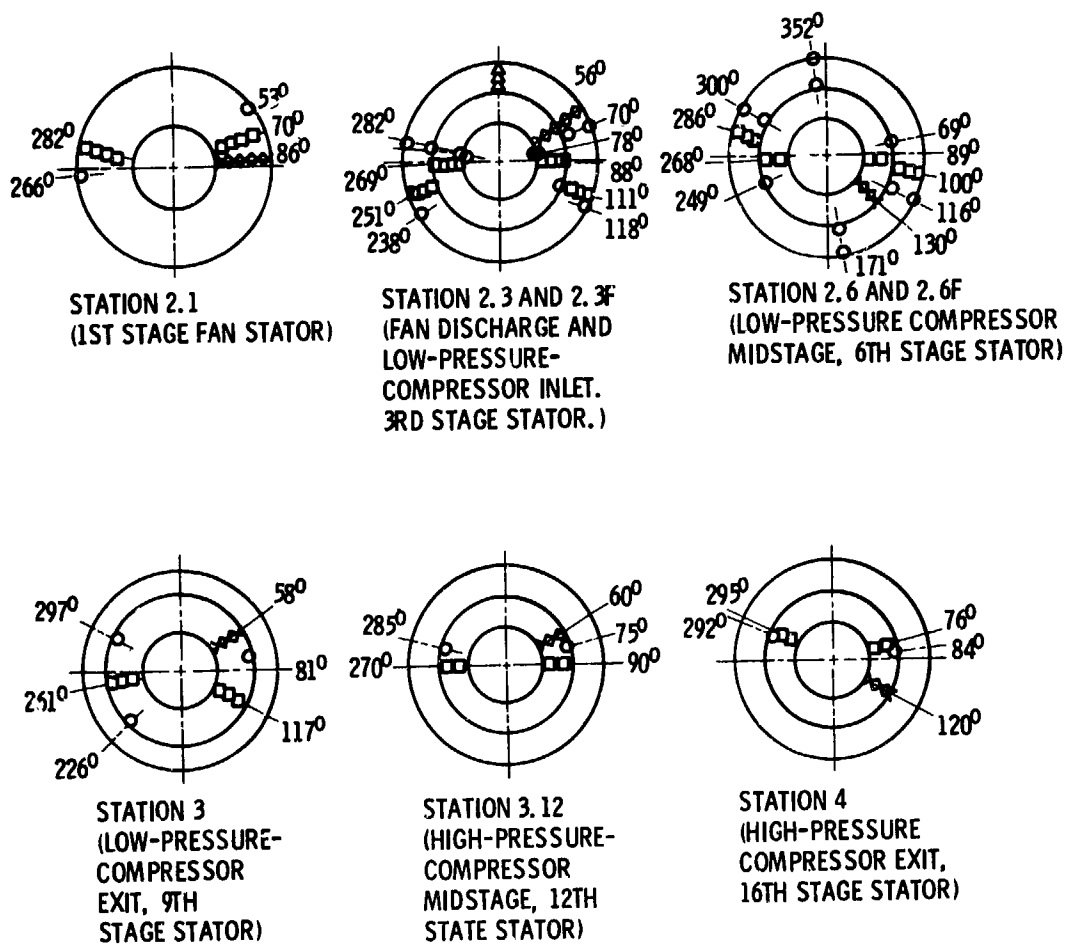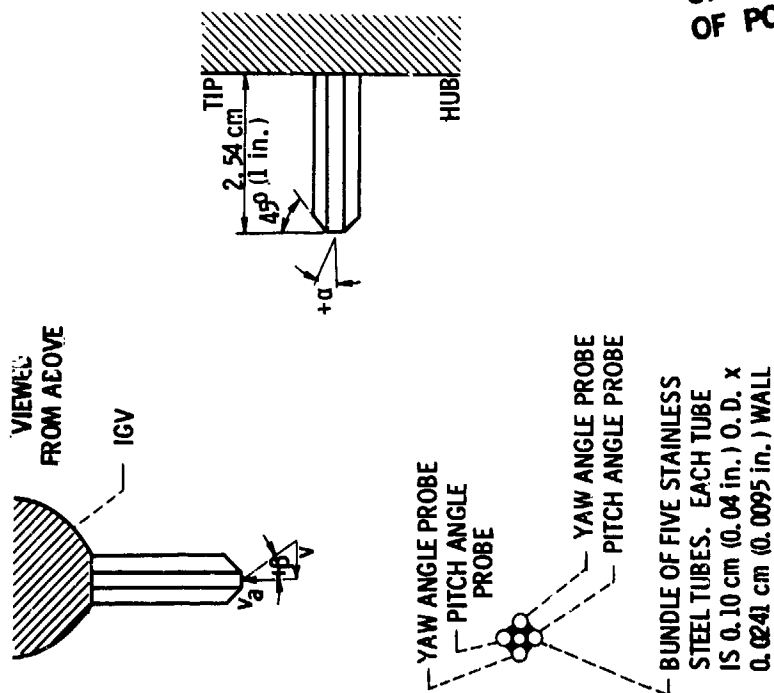(1ST STAGE FAN STATOR)

STATION 2.3 AND 2.3F
(FAN DISCHARGE AND
LOW-PRESSURE-
COMPRESSOR INLET.
3RD STAGE STATOR.)

STATION 2.6 AND 2.6F
(LOW-PRESSURE COMPRESSOR
MIDSTAGE, 6TH STAGE STATOR)

STATION 3
(LOW-PRESSURE-
COMPRESSOR
EXIT, 9TH
STAGE STATOR)

STATION 3.12
(HIGH-PRESSURE-
COMPRESSOR
MIDSTAGE, 12TH
STATE STATOR)

STATION 4
(HIGH-PRESSURE
COMPRESSOR EXIT,
16TH STAGE STATOR)

Figure 3. - Concluded.

(b) BOUNDARY LAYER YAW ANGLE PROBE.

Figure 4. - Continued.

(a) PITCH-YAW PROBE MOUNTED ON IGV.

Figure 4. - Flow angle instrumentation.

Figure 5. – Inlet duct circumferential profiles with inlet flow distortion for TF30-P-3 at N_1 = 8600 rpm and 0.5 RNI.

(a) TOTAL PRESSURE.

(b) STATIC PRESSURE.

(c) CORRECTED MASS FLOW.

(d) TOTAL TEMPERATURE.

(e) STATIC PRESSURE.

(f) CORRECTED MASS FLOW.

TOTAL TEMPERATURE DISTORTION

TOTAL PRESSURE DISTORTION

CIRCUMFERENTIAL POSITION, deg

STATION

| | A, 1 | IGV |

STAINLESS STEEL TUBE
0.102 cm (0.04 in.) O.D. x
0.017 cm (0.0065 in.) WALL

PROBE	D	E	NO. REQUIRED
TIP	0.51 cm (0.20 in.)	1.02 cm (0.40 in.)	1
HUB	0.38 cm (0.15 in.)	0.64 cm (0.25 in.)	1

SECT. C-C

GUSSET PLATE

SECTION B-B

YAW ANGLE PROBES

SECTION A-A

BOTTOM VIEW

(c) TIP AND HUB BOUNDARY LAYER YAW PROBES.

Figure 4. – Concluded.

Figure 6. - Static pressure distortion at outer wall between screen and IGV for TF30-P-3 at 0.5 RNI and N_1 = 8600 rpm.

Figure 7. - Comparison of predicted and measured inlet static pressure distortion for TF30-P-3 at N_1 = 8600 rpm and 0.5 RNI.
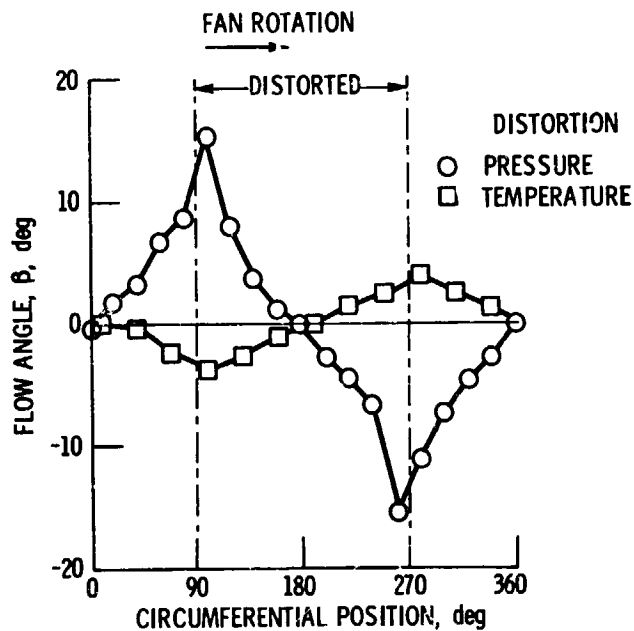
FAN ROTATION

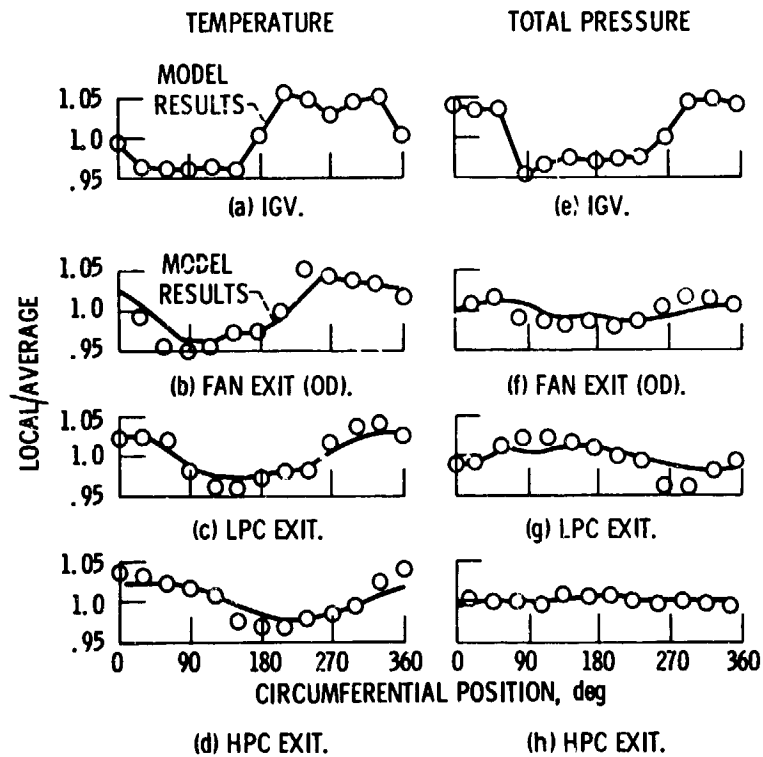Figure 8. - Angle of distorted flow entering the fan IGV of TF30-P-3 at N_1 = 8600 rpm and 0.5 RNI.

TEMPERATURE   TOTAL PRESSURE

(a) IGV.   (e) IGV.

(b) FAN EXIT (OD).   (f) FAN EXIT (OD).

(c) LPC EXIT.   (g) LPC EXIT.

(d) HPC EXIT.   (h) HPC EXIT.

Figure 9. - Comparison of measured and predicted internal compressor profiles for combined pressure and temperature distortions - TF30-P-3 at N_1 = 8600 rpm and 0.5 RNI.
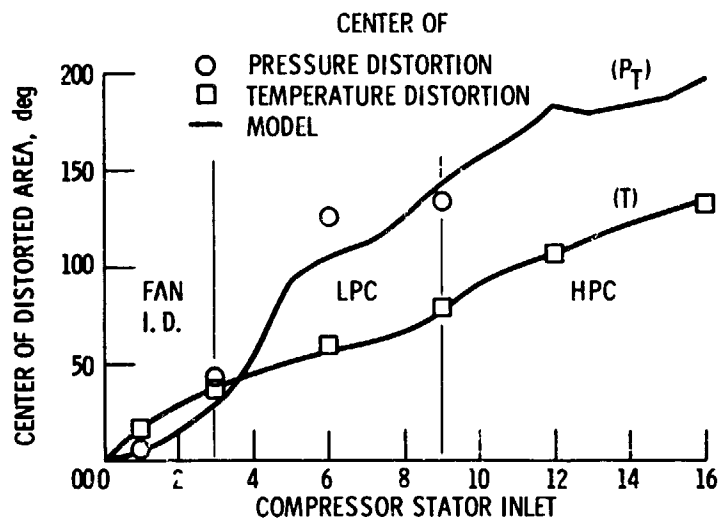
CENTER OF
O   PRESSURE DISTORTION
□   TEMPERATURE DISTORTION
—   MODEL

Figure 10. - Predicted swirl of tot.; pressure and temper-
ature distorted flow passing through compressor system
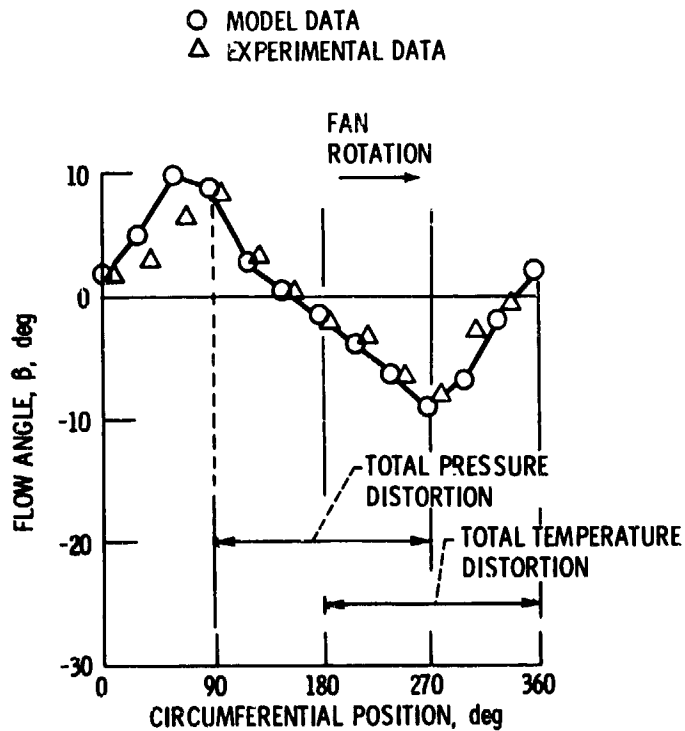of TF30-P-3 at 0.5 RNI and N_1 = 8600 rpm.

O   MODEL DATA
△   EXPERIMENTAL DATA

Figure 11. - Comparison of model and experimental
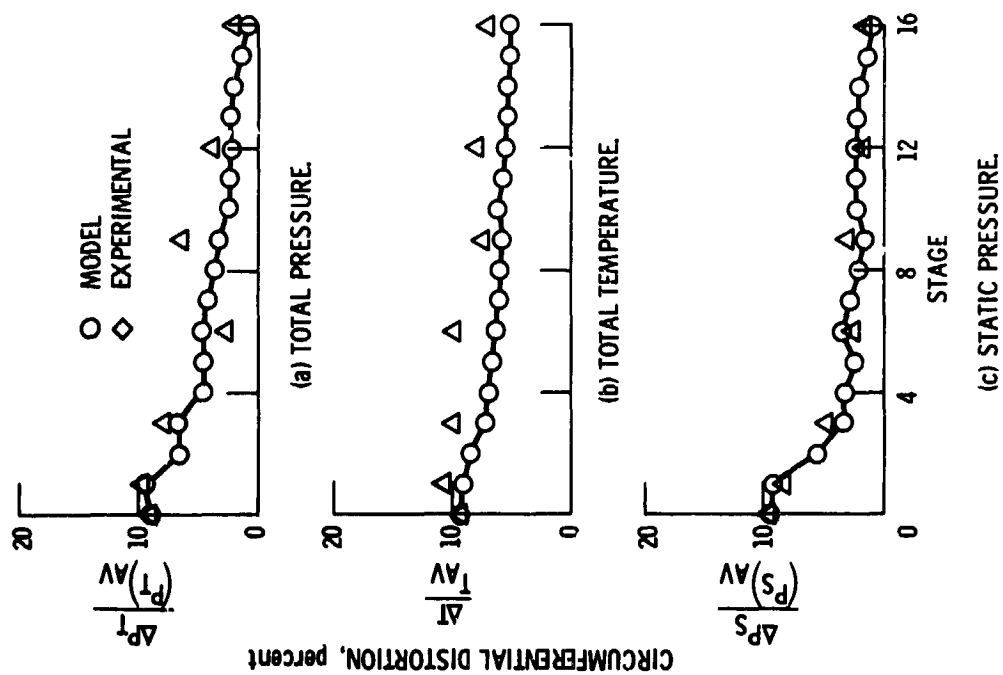approach angles for a complex flow distortion.
N_1 = 8600 rpm, 0.5 RNI.

Figure 13. - Effect of relative position on attenuation of combined P and T distortions for TF30-P-3 at N_1 = 8600 rpm and 0.5 RNI.

Figure 12. - Attenuation of distortion by TF30-P-3 compression system for combined P and T inlet distortion at N_1 = 8600 rpm and 0.5 RNI.
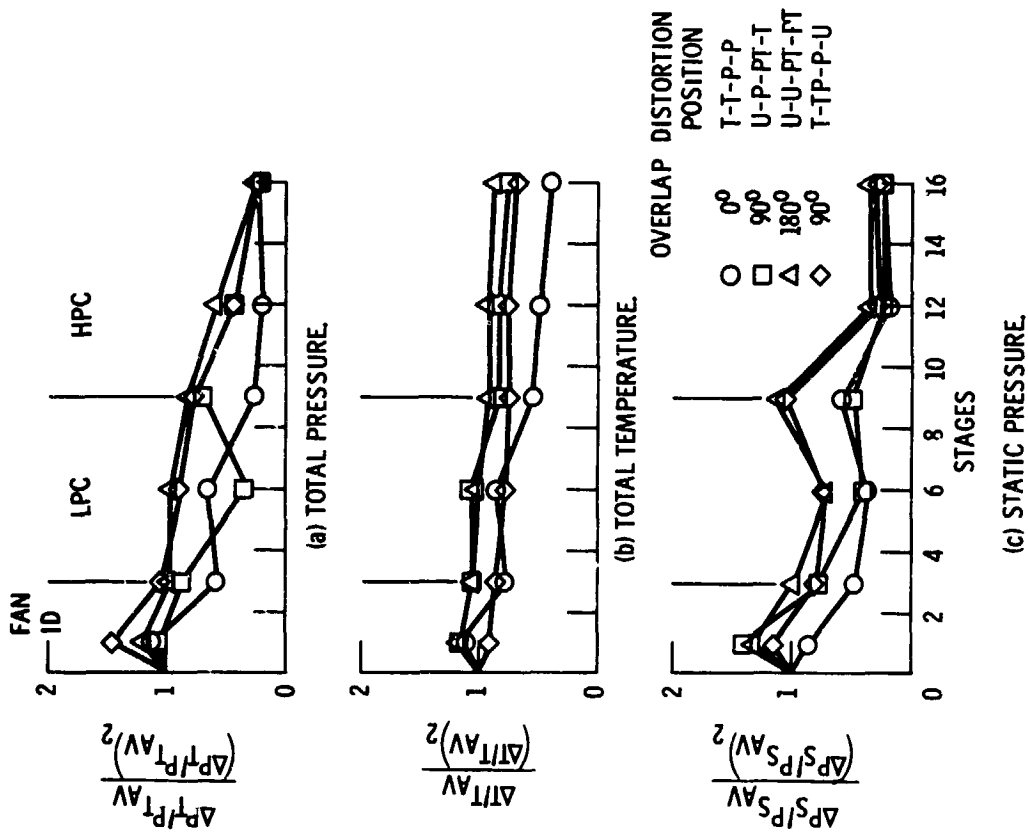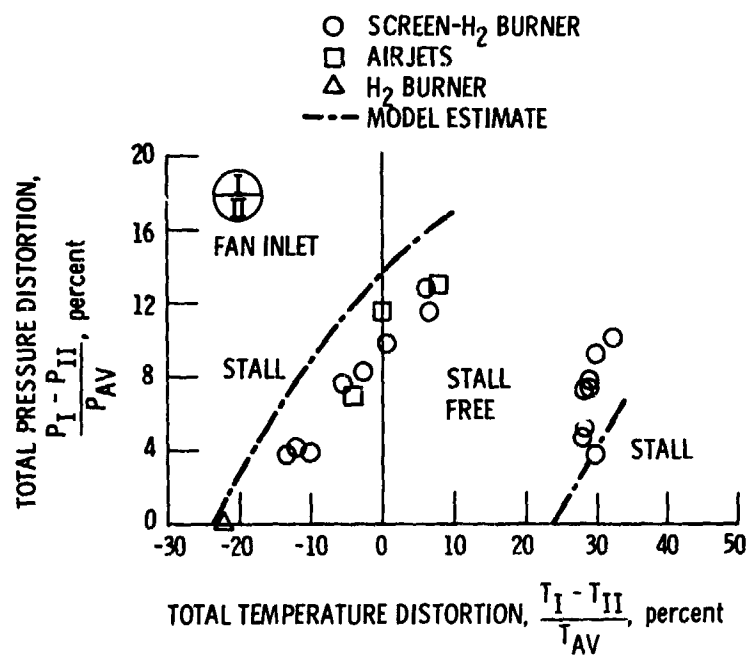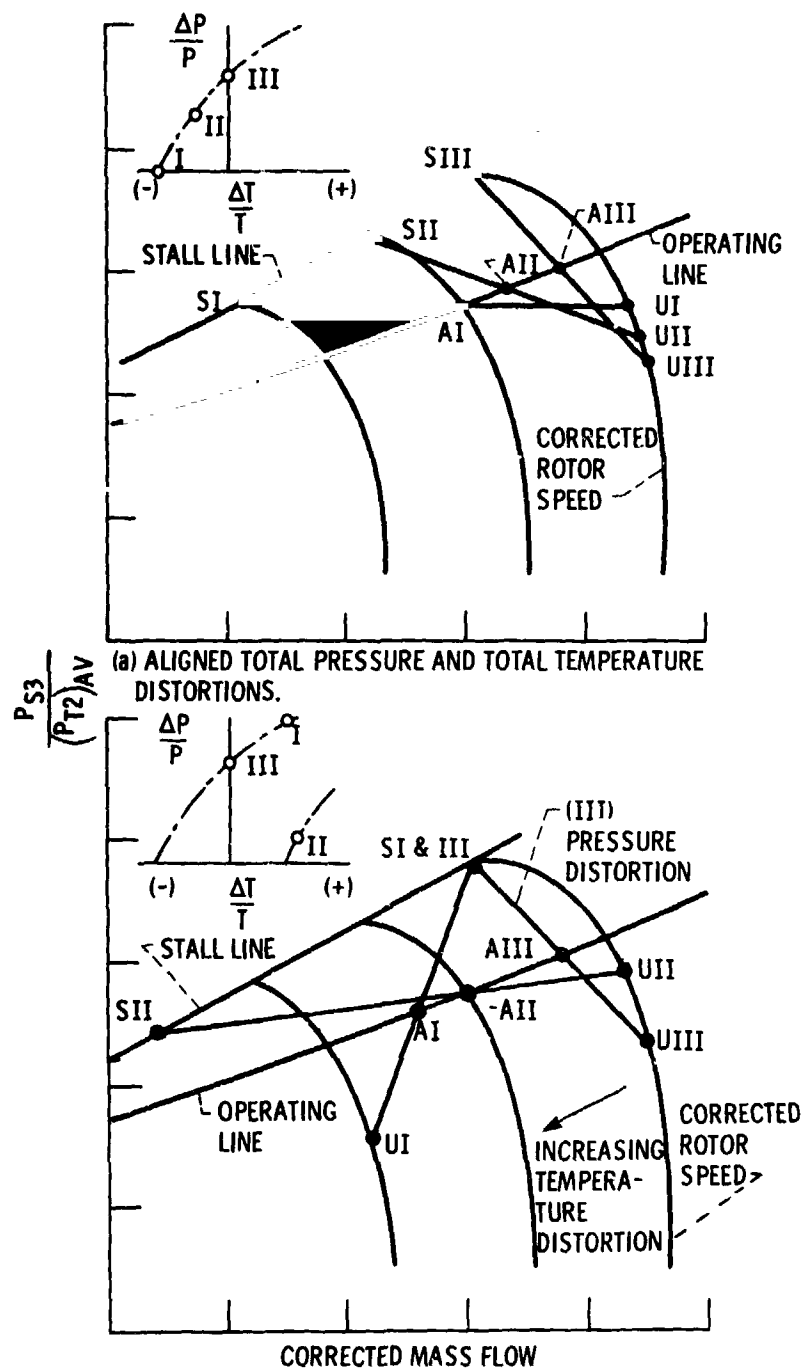
Figure 14. - Effect of relative position on limiting distortion for combined P and T distortions for TF30-P-3 at N_1 = 8600 rpm and 0.5 RNI.

(a) ALIGNED TOTAL PRESSURE AND TOTAL TEMPERATURE
DISTORTIONS.

(b) OPPOSED TOTAL PRESSURE AND TOTAL TEMPERATURE
DISTORTIONS.

Figure 15. – Simple parallel compressor model of combined
P & T distortions.

1. Report No. NASA TM-79136	2. Government Accession No.	3 Recipient's Catalog No

4. Title and Subtitle

COMBINED PRESSURE AND TEMPERATURE DISTORTION EFFECTS ON INTERNAL FLOW OF A TURBOFAN ENGINE

5 Report Date
6. Performing Organization Code

7. Author(s)

W. M. Braithwaite and Ronald H. Soeder

8 Performing Organization Report No E-9984
10 Work Unit No

9. Performing Organization Name and Address

National Aeronautics and Space Administration
Lewis Research Center
Cleveland, Ohio 44135

11. Contract or Grant No
13. Type of Report and Period Covered

12. Sponsoring Agency Name and Address

National Aeronautics and Space Administration
Washington, D.C. 20546

Technical Memorandum

14. Sponsoring Agency Code

15. Supplementary Notes

16. Abstract

An experimental investigation was conducted, and is herein reported, to obtain an additional data base for improving and verifying a computer simulation developed by an engine manufacturer. The multisegment parallel compressor simulation was designed to predict the effects of steady-state circumferential inlet total-pressure and total-temperature distortions on the flows into and through a turbofan compression system. It also predicts the degree of distortion that will result in surge of the compressor. Previous investigations have dealt mainly with the effects of total-pressure distortions. The investigation reported herein deals with the effect of combined 180° "square-wave" distortion patterns of total pressure and total temperature in various relative positions. The observed effects of the combined distortion on a unitary bypass ratio turbofan engine are presented in terms of total and static pressure profiles and total temperature profiles at stations ahead of the IGV (inlet guide vanes) as well as through the fan-compressor system. These observed profiles are compared with those predicted by the complex multisegment model. The effects of relative position of the two components comprising the combined distortion on the degree resulting in surge are also presented. Certain relative positions required less combined distortion than either a temperature or pressure distortion by itself.

17. Key Words (Suggested by Author(s))

Turbofan engine
Combined distortion
Distortion computer simulation

18 Distribution Statement

Unclassified - unlimited
STAR Category 07

19. Security Classif. (of this report) Unclassified	20. Security Classif. (of this page) Unclassified	21. No. of Pages	22. Price*